

A high-throughput thermoelectric power-factor screening tool for rapid construction of thermoelectric property diagrams

M. Otani,^{a)} N. D. Lowhorn, P. K. Schenck, W. Wong-Ng, and M. L. Green
Materials Science and Engineering Laboratory, National Institute of Standards and Technology,
Gaithersburg, Maryland 20899, USA

K. Itaka and H. Koinuma
Graduate School of Frontier Sciences, The University of Tokyo, Kashiwa 277-8568, Japan

(Received 5 July 2007; accepted 1 September 2007; published online 24 September 2007)

The authors have developed a high-throughput screening tool that maps out thermoelectric power factors of combinatorial composition-spread film libraries. The screening tool allows one to measure the electrical conductivity and Seebeck coefficient of over 1000 sample points within 6 h. Seebeck coefficients of standard films measured with the screening tool are in good agreement with those measured by traditional thermoelectric measurement apparatus. The rapid construction of thermoelectric property diagrams is illustrated for two systems: (Zn, Al)-O binary composition-spread film on Al₂O₃ (0001) and (Ca, Sr, La)₃Co₄O₉ ternary composition-spread film on Si (100). © 2007 American Institute of Physics. [DOI: 10.1063/1.2789289]

In recent years, there has been considerable interest in thermoelectric devices for large scale industrial applications, including all solid-state electric refrigeration, and power generation from waste heat.¹ High efficiency thermoelectric devices require materials with large dimensionless figures of merit ($ZT = S^2 \sigma \kappa^{-1} T$, where S is Seebeck coefficient, σ is electrical conductivity, κ is thermal conductivity, and T is absolute temperature). The quest for efficient thermoelectric materials continues to be a challenge and has remained an active area of research. Synthesis of solid solutions is an efficient approach to improve ZT not only by optimizing carrier concentration² but also by increasing carrier mobility by lattice deformation³ and reducing thermal conductivity by the alloying effect.⁴ Numerous studies on solid solution quaternary or higher component systems [i.e., CeFe_{4-x}Co_xSb₁₂,⁵ Zr_{0.5}Hf_{0.5}Ni_{0.5}Pd_{0.5}Sn_{0.99}Sb_{0.01},⁶ (Ca, Bi, Sr)₃Co₄O₉,³ and (Ca, Sr, Ba)(Ti, Nb)O₃ (Ref. 7)] have been reported. However, in order to investigate the thermoelectric properties as a function of composition in these complicated systems, fabrication and measurement based on a one-composition-at-a-time approach are too time consuming. The composition-spread approach (a state-of-the-art combinatorial methodology) is a powerful and efficient technique for studying multicomponent systems. This method involves fabricating “film libraries” with continuously varying compositions between two or three different materials on a substrate, followed by evaluating the film libraries with high-throughput screening tools;^{8–10} without an appropriate high-throughput screening tool, we would not be able to correlate material properties with composition.^{11,12} The development of a high-throughput screening tool that can evaluate the thermoelectric power factor ($S^2 \sigma$), a preliminary figure of merit for thermoelectric materials, of composition-spread film libraries is therefore a critical need. Although there exist reports in the literature of thermoelectric screening tools, one is applicable only for bulk samples¹³ and the other is restricted to measurement of a maximum of ten sample points.¹⁴ The goal of this paper is to report our recent development of a high-throughput thermoelectric screening tool

that can be used to measure electrical conductivity and Seebeck coefficient of over 1000 sample points within 6 h, and to demonstrate rapid construction of thermoelectric property diagrams.

The thermoelectric screening tool consists of a probe to measure electrical conductivity and Seebeck coefficient, and an automated translation stage to move the probe in the x - y - z directions. Measurements are fully automated by a laptop computer. The measurement probe consists of four spring probes, two thermometers, a heater, two insulators (Kapton¹⁵ tapes or Al₂O₃ plates), and two copper plates (Fig. 1). To achieve accurate Seebeck coefficient measurement, a spring probe is directly placed on each copper plate to ensure low thermal resistance between the probe and the copper plate. The other spring probe is attached to the insulator. The four probes are arranged in a square array, and the distance between the probes is 1 mm. A thermometer is attached to each copper plate, but a heater is attached to only one of the copper plates. The measurement probe and sample stage are placed inside a protective case to stabilize the temperature of the probe. Electrical conductivity is measured by the conventional four-probe method by placing four spring probes on the sample, sending a fixed current through two probes, and measuring the voltage across the other two. The Seebeck coefficient is defined as the ratio of voltage (ΔV) and tem-

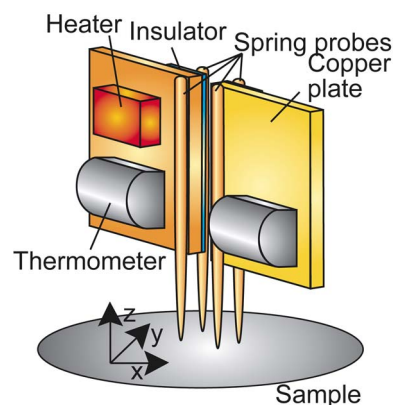


FIG. 1. (Color online) Schematic diagram of measurement probe to measure electrical conductivity and Seebeck coefficient.

^{a)}Electronic mail: motani@nist.gov

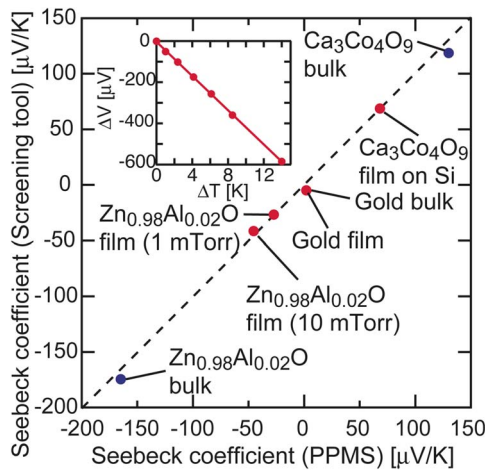


FIG. 2. (Color online) Comparison between Seebeck coefficients measured on several samples, including bulk and film, with our screening tool and a thermal transport option of physical property measurement system (PPMS). The bulk samples are gold foil, polycrystalline $\text{Zn}_{0.98}\text{Al}_{0.02}\text{O}$, and polycrystalline $\text{Ca}_3\text{Co}_4\text{O}_9$. The film samples fabricated by pulsed laser deposition are gold film, $\text{Ca}_3\text{Co}_4\text{O}_9$ film, and two $\text{Zn}_{0.98}\text{Al}_{0.02}\text{O}$ films grown at 1.3 and 13 Pa. Broken line indicates Seebeck coefficients measured by the screening tool and PPMS are identical. (Inset) ΔV of a $\text{Zn}_{0.98}\text{Al}_{0.02}\text{O}$ film fabricated at an oxygen pressure of 1.3 Pa as a function of ΔT .

perature (ΔT) at two points. ΔV is obtained by holding one probe at temperature T , heating the other to $T + \Delta T$, and measuring the voltage across the two. It takes 20 s to measure both the electrical conductivity and Seebeck coefficient for each sample point. Thus, we can measure electrical conductivity and Seebeck coefficient for over 1000 sample points within 6 h. The detailed measurement procedure will be described in another paper.¹⁶ In this paper, all Seebeck coefficient measurements were conducted at room temperature and at $\Delta T = 4.1$ K.

In order to estimate the accuracy of our screening tool, we compared the Seebeck coefficients of several bulk and film samples using our screening probe and a traditional one-measurement-at-a-time system [physical property measurement system (PPMS), Quantum Design,¹⁵ with a thermal transport option at room temperature]. As seen in Fig. 2, measurements using these two instruments are in excellent agreement. The inset of Fig. 2 shows the ΔV of a $\text{Zn}_{0.98}\text{Al}_{0.02}\text{O}$ film as a function of ΔT . The trace fits well to a linear function and the offset is insignificant. These results suggest that the scanning probe is reliable and is sufficiently accurate as a screening tool for Seebeck coefficients of combinatorial samples.

We demonstrated the high-throughput screening of Seebeck coefficient and electrical conductivity using binary (Zn, Al)O and ternary (Ca, Sr, La)₃Co₄O₉ composition-spread films. The composition-spread films were fabricated with a pulsed laser deposition system by the continuous-composition-spread technique.^{10,17} To fabricate the (Zn, Al)-O binary composition-spread film, a ZnO film was first deposited by ablation of a ZnO target using a KrF excimer laser at 800 °C with an oxygen pressure of 13 Pa on a 50 mm Al₂O₃(0001) wafer. The resulting film had a thickness distribution, the center of which is away from that of the substrate. The thickness at the center of the thickness distribution corresponded to 1 ML of ZnO. The substrate was then rotated 180° and a $\text{Zn}_{0.98}\text{Al}_{0.02}\text{O}$ film was deposited. This process was repeated a few hundred times to obtain a

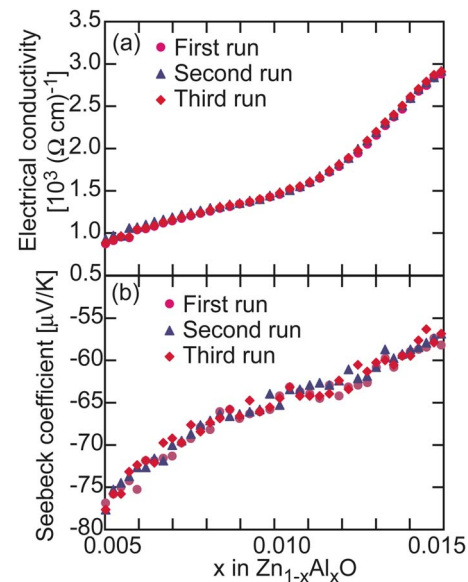


FIG. 3. (Color online) (a) Electrical conductivity and (b) Seebeck coefficient of $\text{Zn}_{1-x}\text{Al}_x\text{O}$ ($0.005 < x < 0.015$) composition-spread thin film as a function of x . Data sets obtained for the same sample three times are plotted in different symbols for estimation of the run-to-run scatter.

composition-spread film of appropriate thickness (more than 200 nm) for thermoelectric measurements. The $(\text{Ca}_{1-x-y}\text{Sr}_x\text{La}_y)_3\text{Co}_4\text{O}_9$ ternary composition-spread film was fabricated using $\text{Ca}_3\text{Co}_4\text{O}_9$, $(\text{Ca}_2\text{Sr})\text{Co}_4\text{O}_9$, and $(\text{Ca}_2\text{La})\text{Co}_4\text{O}_9$ targets at 750 °C with an oxygen pressure of 80 Pa on a 75 mm Si (100) wafer.

To estimate the composition and the total thickness of the composition-spread film, reference single layer films of the constituents of the above compositional spread films [i.e., (Zn, Al)-O, ZnO, $\text{Ca}_3\text{Co}_4\text{O}_9$, $(\text{Ca}_2\text{Sr})\text{Co}_4\text{O}_9$, and $(\text{Ca}_2\text{La})\text{Co}_4\text{O}_9$] were fabricated under the same conditions as those of the composition-spread films. Since the electrical resistance of a thin film is inversely proportional to its thickness, the relative thickness for each point of a single layer film can be evaluated by the four-probe method with the screening tool. The thickness of the thickness center was measured by a wet-etching technique and by an atomic force microscope. From the thickness distributions of all single layer films, we can estimate the composition and the total thickness of the composition-spread film.¹⁷

Figures 3(a) and 3(b) give the electrical conductivity and Seebeck coefficient of the $(\text{Zn}_{1-x}\text{Al}_x)\text{-O}$ composition-spread film measured by the screening tool. As the Al content increases, the electrical conductivity also increases, while the absolute value of Seebeck coefficient decreases. This trend is consistent with that previously seen for Al-doped ZnO bulk samples.¹⁸ In general, as the carrier concentration increases in a material, the electrical conductivity increases, while the Seebeck coefficient decreases. We also found that electrical conductivity of the film is higher, and the absolute value of Seebeck coefficient is lower than those of bulk samples.¹⁸ This result may be caused by carriers generated by oxygen vacancies. In order to estimate the run-to-run consistency, we repeated the same measurement on the same sample three times [Fig. 3(b)]. The results indicate that the run-to-run consistency is sufficient for screening of combinatorial samples.

Figures 4(a) and 4(b) illustrate the electrical conductivity and Seebeck coefficient of the $(\text{Ca}_{1-x-y}\text{Sr}_x\text{La}_y)_3\text{Co}_4\text{O}_9$ ternary composition-spread film measured with the screening

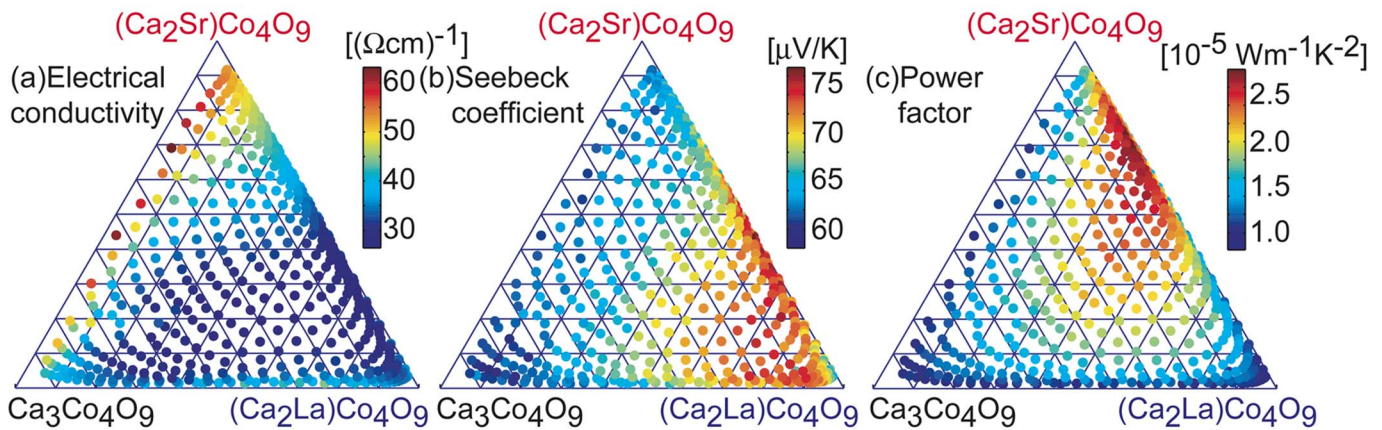


FIG. 4. (Color online) (a) Electrical conductivity, (b) Seebeck coefficient, and (c) power factor of the composition-spread $(\text{Ca}_{1-x-y}\text{Sr}_x\text{La}_y)_3\text{Co}_4\text{O}_9$ film ($0 < x < 1/3$ and $0 < y < 1/3$).

tool. It is seen that as one substitutes La^{3+} for Ca^{2+} , the electrical conductivity decreases and the Seebeck coefficient increases. This is because substitution of trivalent La^{3+} for divalent Ca^{2+} is expected to decrease the hole concentration.¹⁹ On the other hand, substitution of Sr^{2+} for Ca^{2+} leads to an increase of electrical conductivity and an insignificant change of the Seebeck coefficient. This is because the substitution of a larger divalent Sr^{2+} cation for a smaller divalent Ca^{2+} cation would not change the carrier concentration, but would effect the carrier mobility via lattice deformation.³ We note that our $\text{Ca}_3\text{Co}_4\text{O}_9$ films on Si (100) wafers have lower Seebeck coefficients than the literature reported values.²⁰ This difference may be attributed to nonstoichiometry of the film. The power factor ($S^2\sigma$) of the $(\text{Ca}_{1-x-y}\text{Sr}_x\text{La}_y)_3\text{Co}_4\text{O}_9$ ternary composition-spread film is also depicted as a conventional ternary diagram [Fig. 4(c)]. It is clear that the power-factor data peaks between the Sr-rich region and the La-rich region. This result is logical since electrical conductivity is high in the Sr-rich region, and Seebeck coefficient is large in the La-rich region.

The current configuration of our screening tool gives rise to three limitations. First, it is difficult to measure materials with low [i.e., $<10^{-1}$ ($\Omega\text{cm})^{-1}$ for a 200 nm thin film] electrical conductivity and low ($<5\mu\text{V/K}$) absolute value of Seebeck coefficient due only to limitations of the homemade current source and voltage meter. Although these limitations do not hamper our ability to screen thermoelectric materials, we could extend our measurement capability by upgrading those two components. Second, the spatial resolution of our screening tool is about 1 mm, corresponding to the distance between two spring probes. If the electrical conductivity of the sample drastically changed over a very short length scale, measurements at a sample point might be affected by its neighbors. Patterning of the continuous library films into discrete dots could solve this problem. Third, measurements can be carried out only at room temperature at present. We plan to develop a modified probe that is capable of high temperature (up to 500 °C) measurement.

In conclusion, we demonstrate that a ternary thermoelectric power-factor diagram can be obtained from only one composition-spread film library within 6 h of measurement using our screening tool. This versatile screening tool, in addition to applying to oxide composition-spread films prepared by the combinatorial pulsed laser deposition method, can also be applied to metal or semiconductor composition-

spread films fabricated by sputtering²¹ or molecular beam epitaxy.²² We believe that the combination of the thermoelectric screening tool and the composition-spread method will enable the acceleration of thermoelectric research.

¹T. M. Tritt and M. A. Subramanian, MRS Bull. 31, 188 (2006).

²C. M. Bhandari and D. M. Rowe, *CRC Handbook of Thermoelectrics*, edited by D. M. Rowe (CRC, Boca Raton, FL, 1995), pp. 43–54.

³I. Matsubara, R. Funahashi, M. Shikano, K. Sasaki, and H. Enomoto, Appl. Phys. Lett. 80, 4729 (2002).

⁴G. S. Nolas, J. Yang, and H. J. Goldsmid, *Thermal Conductivity*, edited by M. Tritt (Springer, Berlin, 2004), pp. 143–144.

⁵B. C. Sales, D. Mandrus, and R. K. Williams, Science 272, 1325 (1996).

⁶Q. Shen, L. Chen, T. Goto, T. Hirai, J. Yang, G. P. Meisner, and C. Uher, Appl. Phys. Lett. 79, 4165 (2001).

⁷M. Yamamoto, H. Ohta, and K. Koumoto, Appl. Phys. Lett. 90, 072101 (2007).

⁸R. B. Van Dover, L. F. Schneemeyer, and R. M. Fleming, Nature (London) 392, 162 (1998).

⁹T. Fukumura, M. Ohtani, M. Kawasaki, Y. Okimoto, T. Kageyama, T. Koida, T. Hasegawa, Y. Tokura, and H. Koinuma, Appl. Phys. Lett. 77, 3426 (2000).

¹⁰H. M. Christen, S. D. Silliman, and K. S. Harchavardhan, Rev. Sci. Instrum. 72, 2673 (2001).

¹¹H. Chang, I. Takeuchi, and X.-D. Xiang, Appl. Phys. Lett. 74, 1165 (1999).

¹²M. Ohtani, T. Fukumura, M. Kawasaki, K. Omote, T. Kikuchi, J. Harada, A. Ohtomo, M. Lippmaa, T. Ohnishi, D. Komiyama, R. Takahashi, Y. Matsumoto, and H. Koinuma, Appl. Phys. Lett. 79, 3594 (2001).

¹³A. Yamamoto, D. Kukuruznyak, P. Ahmet, T. Chikyow, and F. S. Ohuchi, Mater. Res. Soc. Symp. Proc. 804, JJ1.4 (2004).

¹⁴K. Itaka, H. Minimi, H. Kawaji, Q. J. Wang, J. Nishi, M. Kawasaki, and H. Koinuma, J. Therm. Anal. Calorim. 69, 1051 (2002).

¹⁵Certain trade names and company products are mentioned in the text or identified in illustrations in order to adequately specify the experimental procedure and equipment used. In no case does such identification imply recommendation or endorsement by National Institute of Standards and Technology.

¹⁶M. Otani, K. Itaka, W. Wong-Ng, P. K. Schenck, and H. Koinuma (unpublished).

¹⁷N. D. Bassim, P. K. Schenck, M. Otani, and H. Oguchi, Rev. Sci. Instrum. 78, 072203 (2007).

¹⁸T. Tsubota, M. Ohtaki, K. Eguchi, and H. Arai, J. Mater. Chem. 7, 85 (1997).

¹⁹D. Wang, L. Chen, Q. Wang, and J. Li, J. Alloys Compd. 376, 58 (2004).

²⁰Y. F. Hu, W. D. Si, E. Sutter, and Q. Li, Appl. Phys. Lett. 86, 082103 (2005).

²¹K.-S. Chang, M. L. Green, J. Suehle, E. M. Vogel, H. Xiong, J. Hattrick-Simpers, I. Takeuchi, O. Famodu, K. Ohmori, P. Ahmet, T. Chikyow, P. Majhi, B.-H. Lee, and M. Gardner, Appl. Phys. Lett. 89, 142108 (2006).

²²F. Tsui and L. He, Rev. Sci. Instrum. 76, 062206 (2005).